Forced Convective Cooling Enhancement of Electronic Package Configurations Through Self-Sustained Oscillatory Flows

J. S. Nigen
Graduate Research Assistant.
Student Mem. ASME

C. H. Amon
Associate Professor.
Mem. ASME

Department of Mechanical Engineering and,
Engineering Design Research Center,
Carnegie Mellon University,
Pittsburgh, PA 15213

Two-dimensional arrangements of electronic packages surface mounted to a printed circuit board represent grooved-channel geometries. For a certain range of Reynolds numbers, these geometries excite and sustain instabilities that are normally damped in planar Poiseuille flows. This results in a bifurcation to a self-sustained oscillatory state, which improves mixing and thereby enhances convective heat transport. Numerical simulations of the flow field and heat transfer characteristics of oscillatory and nonoscillatory flows for five grooved channels are presented. Additionally, the numerically obtained flow field corresponding to a suspended electronic package is analyzed. The extent of heat transfer enhancement is gauged through direct comparison to results corresponding to the steady-flow regime. Local heat transfer coefficients are determined and used to calculate the temperature distribution within a surface-mounted package. Moreover, the importance of using locally-defined instead of spatially-averaged heat transfer coefficients for thermal design and analysis of electronic packages is discussed.

Introduction

The rapid increase in the ability to design and produce chips with high-gate densities has dramatically improved the performance of electronic components. However, higher heat dissipation per unit area is required to maintain acceptable operating temperatures. The well-known exponential relationship between the junction temperature and the failure acceleration factor (U.S.A.F. Rome Air Development Center, 1982) justifies reduction of these temperatures as much as practically and economically possible. Juxtaposed with these reliability issues are market concerns, necessitating that cooling configurations be non-obtrusive to a work environment. Maintenance of an acceptable work environment places restrictions upon the size and acoustic output of any cooling configuration. Such concerns obviously favor natural convection as opposed to forced convection because of the noise produced by a forcing device (e.g., a fan). Unfortunately, many situations call for more convective heat transport than that possibly rendered through natural convection. The thermal designer must then resort to forced convection and, therefore, the addition of a forcing device.

One way to improve convective heat transfer is to diminish the thermal resistance of the boundary layer by reducing its thickness (Kays and Crawford, 1980). For turbulent flows, this argument suggests that thermal designers should select a forcing device that produces Reynolds number flows high enough to achieve required convective heat transfer rates. However, in compact channels, such as those encountered in electronics cooling, the length scale by which the Reynolds number is defined can be of the order of 1 cm. Therefore, the velocities required to generate turbulent Reynolds numbers can be prohibitive. Alternatively, the thickness of the thermal boundary layer may be reduced through surface segmentation. As in the grooved-channel geometry, shown in Fig. 1, the boundary layers would have to restart at the beginning of each elevated section. This geometry is naturally present in electronic board configurations with surface-mounted components.

An unfortunate consequence of the groove-channel geometry is the creation of a shear layer between the channel and the groove flows (Figs. 2(*a*) and (*b*)). In a certain range of Reynolds numbers, the shear layer acts as a barrier, significantly reducing or eliminating convective exchange of fluid between the groove and channel. In such cases, heat is exchanged between the groove and channel flows through dif-

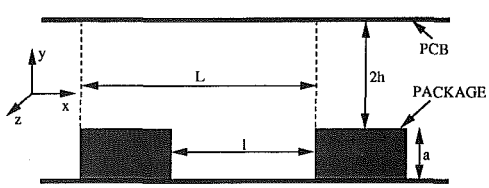

Fig. 1 Schematic of the grooved-channel geometry

Contributed by the Electrical and Electronic Packaging Division for publication in the JOURNAL OF ELECTRONIC PACKAGING. Manuscript received by the EEPD December 10, 1992; revised manuscript received June 28, 1993. Associate Technical Editor: W. Black.

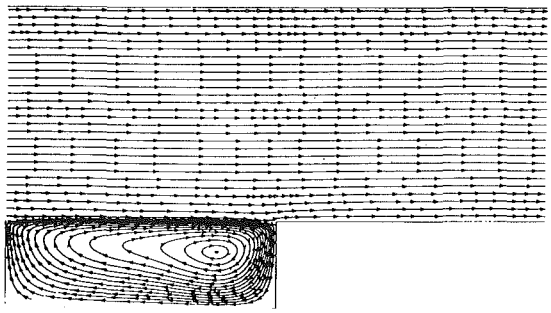

Fig. 2(*a*)

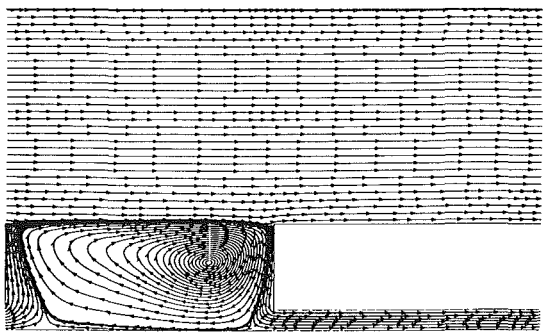

Fig. 2(*b*)

Fig. 2 Streamlines showing the flow pattern and vortex structure of the steady flow regime at Re = 375 for (*a*) Smount 1 and (*b*) Ivtpga geometries

fusion. Essentially, the fluid in the groove is trapped and merely recirculates, increasing in temperature and diminishing in its ability to remove heat. Many solutions have been proposed which disrupt or remove the shear layer and thereby increase mixing of the fluid. These may be classified as either active or passive techniques.

Active destabilization employs external flow modulation to disrupt the shear layer and increase communication between the groove and channel flows (Sobey, 1980; Ghaddar et al., 1986a; Greiner, 1991; and Azar, 1992). The effectiveness of active destabilization is directly related to the proper selection of the modulation frequency. Alternatively, passive flow destabilization may utilize obstacles such as cylinders that are placed in the channel. These obstacles periodically shed vortices that serve to disrupt the shear layer and improve mixing (Ratts et al., 1988; Karniadakis, 1988; and Suzuki, 1991). Another passive approach makes use of geometrically induced instabilities to disrupt the shear layer. This is achieved by selecting the flow rate to excite and sustain normally the damped Tollmien-Schlichting waves present in planar Poiseuille flow (Ghaddar et al., 1986b; Amon and Mikic, 1990). The shear layer is disrupted and mixing is improved through the interaction of Tollmien-Schlichting waves in the channel with recirculating fluid in the groove. The resulting rates of convective heat transfer are comparable to those of higher Reynolds numbers, namely, in the turbulent flow regime. However, the lower velocities serve to reduce acoustic output and the required pumping power (Amon, 1992).

Although all the above methods improve mixing and therefore augment heat removal, the passive methods are perhaps more appropriate to electronics cooling applications because they eliminate the added costs and complexities of an active system (Leonard, 1990). Therefore, one of the objectives of this paper is to demonstrate the effectiveness of passive flow destabilization in reducing the junction temperature of a sample electronic package, through the appropriate selection of the Reynolds number range and geometric dimensions. Moreover, the significance of specifying a spatially-varying heat transfer coefficient will be demonstrated.

Problem Formulation

The geometric domain to be examined is the grooved-channel geometry (Fig. 1), which is infinite in depth, z, rendering the problem two-dimensional. The incoming velocity field is considered to be periodically fully developed in the streamwise direction, x, and the fluid is assumed to be incompressible with invariant physical properties.

The continuous problem is formulated using the Navier-Stokes equations and conservation of both mass and energy. The continuity, Navier-Stokes expressed in rotational form, and energy equations are,

$$\nabla \cdot \mathbf{v} = 0 \tag{1}$$

$$\frac{\partial \mathbf{v}}{\partial t} = \omega \times \mathbf{v} - \frac{1}{\rho} \nabla \left(p + \frac{\rho \mathbf{v}^2}{2} \right) + \nu \nabla^2 \mathbf{v} \tag{2}$$

$$\frac{\partial T}{\partial t} = \alpha_{\text{th}} \nabla^2 T - \mathbf{v} \cdot \nabla T \tag{3}$$

The numerical approach is that of direct simulation, using initial value solvers. Additionally, all coupling between the momentum and energy equations is through the convective terms in Eq. (3). In particular, the temperature is passive and does not drive the flow, and viscous dissipation does not enter as a source term in the energy equation.

The temporal discretization is accomplished using finite differences, while the spatial discretization is conducted using the spectral element technique (Patera, 1984; Korczak and Patera, 1986). The spectral element technique is a high-order, weighted-residual technique that combines the geometric flexibility of finite element methods with the accuracy and rapid convergence of spectral methods. The domain is decomposed into a series of quadrangular sub-domains or elements, which are isoparametrically mapped from the physical into the computational space. A spectral element mesh for the grooved-channel geometry depicting the element subdivision is displayed in Fig. 3(*a*) and including the collocation points in Fig. 3(*b*).

Nomenclature

a = groove depth (Fig. 1)
c = eigenvalue
D = differential operator
h = half-channel height (Fig. 1)
l = groove width (Fig. 1)
L = periodic length (Fig. 1)
Nu = Nusselt number
p = pressure
Pr = Prandtl number
Re = Reynolds number = Vh/ν
Re_c = critical Reynolds number
Re_{cp} = critical Reynolds number for planar Poiseuille flow
t = time
T = temperature
T_p = period of self-sustained oscillatory velocity
u, v = velocity components in the x- and y- directions
V = maximum channel velocity
α = streamwise wavenumber
α_{th} = thermal diffusivity
ρ = density
ν = kinematic viscosity
ω = vorticity
ω_{TS} = Tollmien-Schlichting frequency
ω_{OF} = frequency of self-sustained oscillatory flow

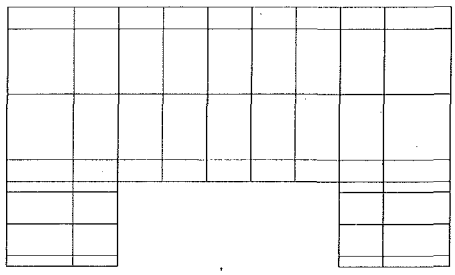

Fig. 3(*a*)

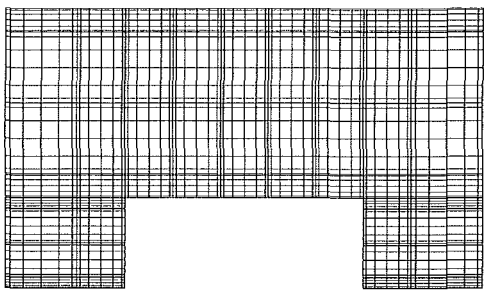

Fig. 3(*b*)

Fig. 3 Spectral element discretization depicting (*a*) macro-elemental discretization and (*b*) collocation points

Using this solution technique, the Navier-Stokes and energy equations are solved to investigate the forced convective phenomena associated with six geometries. The first three, Groove 1, Groove, 2, and Groove 3, differ only in groove width, i.e., separation between packages. The next two, Smount 1 and Smount 2, represent surface-mounted components with different heights, leading to varying groove depths. These geometries are studied with the intent of investigating the relationship between the behavior of the fluid and the heat transfer coefficients. The remaining geometry, Ivtpga, is an InVerTed Pin Grid Array geometry and is selected to explore the importance of communication underneath a package.

Linear Stability

A mathematical model is formulated to follow the evolution of disturbances introduced into a laminar flow and determine whether they decay, grow, or remain fixed in amplitude. An assumption is made which consists of prescribing that the magnitude of the characteristics associated with the disturbances are *small*, enabling the elimination of any quadratic combinations of disturbance components (Schlichting, 1979). After some manipulation, the resulting expression is the Orr-Sommerfeld equation (Eq. (4)),which represents the Navier-Stokes equation linearized about a steady, fully-developed, planar Poiseuille velocity profile (Drazin and Reid, 1981).

$$\frac{1}{i\alpha \mathrm{Re}}(D^2-\alpha^2)^2\phi = (U-c)(D^2-\alpha^2)\phi - (D^2U)\phi \qquad (4)$$

For any specified values of α and Re, there exists a corresponding infinite discrete spectrum of eigenvalues, c, yielding nontrivial solutions. Each eigenvalue has an associated velocity of propagation or phase speed, Real(c), and growth rate, Im(c), respectively. The eigenvalue with the maximum growth rate physically corresponds to the least-stable mode, usually referred to as *Tollmien-Schlichting waves.*

In planar channel flow, the growth rate is found to be negative for Reynolds numbers less than 5772. This indicates that a small disturbance introduced into such a flow will decay in time, resulting in a time-independent parallel flow. In the grooved-channel geometry, the periodic presence of elevated sections will serve to sustain the Tollmien–Schlichting waves, resulting in finite-amplitude oscillatory flows. These sustained oscillations occur at lower Reynolds numbers (of the order O(100)) than those indicated by the linear theory for the corresponding planar channel flows.

Time-Periodic Flows

According to linear hydrodynamic stability analysis, a critical Reynolds number, Re_c, may exist beyond which the flow is no longer stable. As previously noted, for the case of planar Poiseuille flows, the Re_{cp} is 5772. In the case of grooved-channel geometries, flows at Reynolds numbers greater than Re_c, i.e., supercritical flows, exhibit traveling waves with amplitudes proportional to $(\mathrm{Re}-\mathrm{Re}_c)^{0.5}$ (Amon and Patera, 1989).

A complex relationship exists between the traveling waves, present in the channel, and the recirculating groove flow. The resulting effect is that the normally stable vortex within the groove undergoes a repetitive pattern of change. A flow that exhibits these characteristics is considered to be in a *time-periodic* state.

An observed consequence of such a time-periodic pattern is a vast increase in the convective exchange of fluid between the channel and groove flows. This is apparent by contrasting the steady flow pattern in Figs. 2(*a*) and (*b*) with the sequence corresponding to a time period of the supercritical flow, as depicted in Figs. 4(*a*) and (*b*). In the first frame ($t = 0$) of the sequence portrayed in Fig. 4(*a*), the traveling waves have induced separation of the shear layer from the upstream package face, thereby, permitting channel fluid to directly enter into the groove. This also results in a compression of the preexisting recirculating zone into the downstream package face, as well as its expansion into the channel.

In the second frame ($t = 7T_p/20$), there exist two main recirculating zones within the groove. One recirculating zone is formed by the channel fluid flowing over the upstream package corner, as in flow over a backstep. This recirculating zone continues to grow and eventually becomes larger than the preexisting recirculating zone, as seen in the third frame ($t = 10T_p/20$). Channel fluid continues to enter into the groove throughout this portion of the progression.

As depicted in the fourth frame ($t = 14T_p/20$), the shear layer has re-established itself across the groove, resulting in the removal of the driving force for the upstream recirculating zone. This effect causes the two recirculating zones to coalesce inside of a single outer shear layer. Furthermore, the upstream portion of the shear layer has expanded into the channel, while the downstream portion is compressed into the groove. This directly exposes the downstream package corner to the channel flow.

Frame five ($t = 18T_p/20$) clearly shows that the two recirculating zones have fully merged. Additionally, the traveling waves are beginning to induce separation of the shear layer from the upstream package corner, but no channel fluid enters into the groove. Frame six ($t = T_p$) demonstrates that the shear layer has been separated from the upstream package face, allowing channel fluid to enter the groove. Frame six completes the sequence and initiates the new one.

This cycle repeats itself in a periodic fashion, allowing for an organized exchange of channel and groove fluid. Additionally, the channel flow does not exhibit the characteristic turbulent velocity profile. This results in less viscous dissipation, leading to lower pumping power requirements for similar heat transfer rates (Amon and Mikic, 1990).

The same basic characteristics of the repetitive flow sequence demonstrated in Figs. 4(*a*) and (*b*) are exhibited for the other geometries. Namely, the separation phenomena associated with the upstream corner and the movement of the preexisting vortex with respect to the channel waves, dictates the flow in the groove. This would indicate the existence of the same fun-

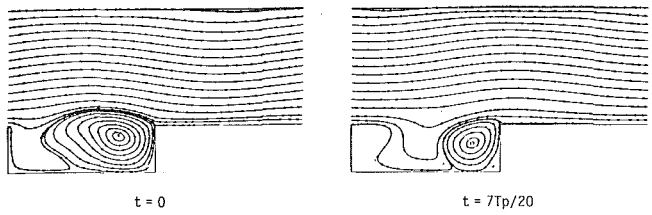

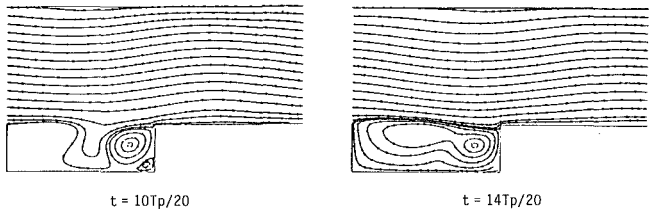

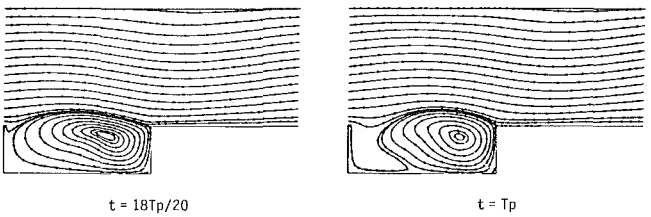

Fig. 4(*a*)

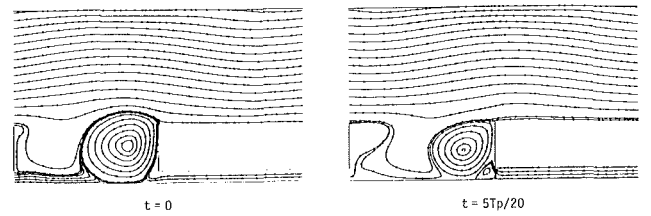

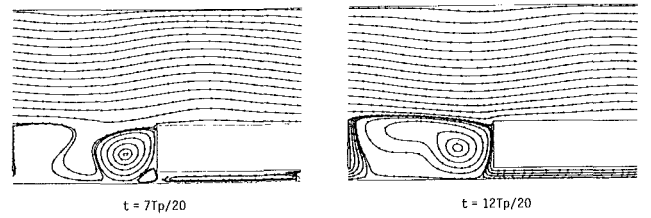

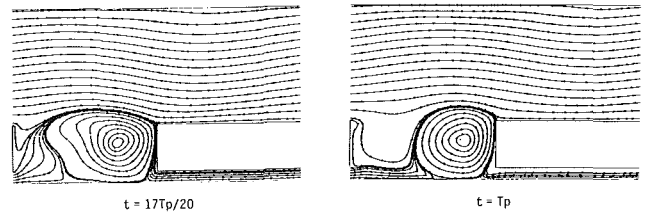

Fig. 4(*b*)

Fig. 4 Sequence of six streamline plots indicating the flow patterns associated with the periodic self-sustained oscillatory flow. Flow comes from left to right; (*a*) Smount 2 at Re = 800 and (*b*) Ivtpga at Re = 800.

damental flow pattern for the relative dimensions of the geometries studied. The major difference among the six geometries is the amplitude of the traveling waves with respect to the Reynolds number. Since unsteadiness leads to better mixing, the desirability of maximum wave amplitude for a given Reynolds number is self evident.

Table 1 Geometric dimensions

	Groove 1	Groove 2	Groove 3
groove depth, a/h	0.715	0.715	0.715
groove width, l/h	2.500	3.000	2.000
channel height, $2h/h$	2.000	2.000	2.000
periodic length, L/h	5.000	5.500	4.500
package width, $(L-l)/h$	2.500	2.500	2.500

Although these simulations are conducted under the assumption of two dimensionality, previous investigators have obtained self-sustained oscillatory flows in three-dimensional representations of similar geometries (Amon and Patera, 1989; Greiner et al., 1990; Amon et al., 1992). Furthermore, a model of a printed circuit board with multiple surface-mounted components was experimentally studied by Garimella and Eibeck (1990). It was demonstrated that a greater variation in convective performance exists in the streamwise than in the spanwise direction across the packages for the geometric and flow rate permutations studied. However, as the spanwise spacing between components is enlarged, the resulting flow patterns would deviate from those presented in this study. This is because the boundary layers growing along the sides of adjacent packages would not become fully developed, leading to the possibility of significant convective transport from these surfaces. Therefore, the results from the two-dimensional study are conservative values and would most closely model the center plane of an equivalent three-dimensional package.

A grooved channel is also realized by attaching a common heat-sink/fin to each successive row of packages. This can offer a performance advantage because of component integration. A thermal designer could specify the dimensional proportions of the common heat sink to optimize the amplitude of the oscillations for a particular flow rate. Therefore, an additional objective of this investigation is to explore the relationship between variations in the geometric proportions of the grooved channel and the amplitude of oscillations.

To investigate the effect of width upon the thermal and fluid performance, three cases are analyzed. The first case, Groove 1, has a groove width equal to that of the component width. The second and third cases, Groove 2 and Groove 3, have larger and smaller groove widths, respectively. The distances, nondimensionalized by half the channel height, are summarized in Table 1.

Simulations are conducted for each geometry for a subcritical and supercritical Reynolds number, i.e., for Reynolds numbers smaller than and greater than Re_c, respectively. To establish a good basis for comparison, the subcritical Reynolds number for all of the Groove cases was selected to be 450, while 375 was selected for the other geometries. The supercritical Reynolds number for each case is as follows: 780 for Groove 1, 700 for Groove 2, 930 for Groove 3, and 800 for Smount 1, Smount 2, and Ivtpga. These Reynolds numbers are chosen because the resulting flow fields (Fig. 5) contain substantial oscillations. However, direct comparisons between each of the supercritical cases must be made with respect to the amplitude of the oscillations, because each has a different critical Reynolds number for bifurcating to a self-sustained oscillatory state.

Oscillograms of the velocity are constructed by storing instantaneous data at a fixed location and subtracting the time-averaged velocity. By taking the discrete Fourier transform of this signal, it is possible to decompose the oscillatory component into its individual Fourier modes. At the critical Reynolds number, the resulting frequency for the least stable mode, ω_{OF}, agrees well with the frequency predicted by the linear theory, ω_{TS}. This suggests that the disturbances are Tollmien-Schlichting in nature and that the numerical simulations are accurate. For each Groove geometry, a summary of the critical

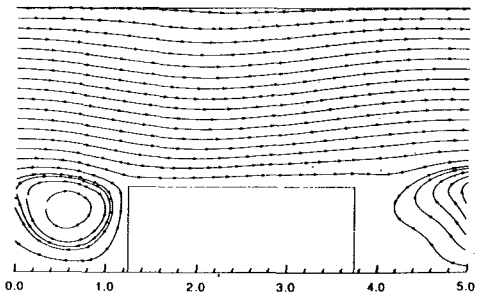

Fig. 5(*a*)

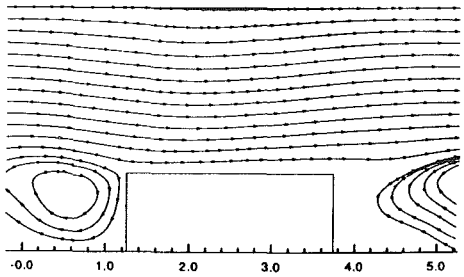

Fig. 5(*b*)

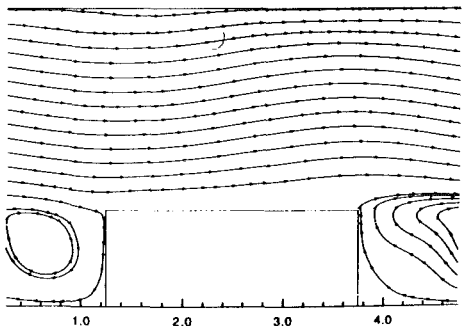

Fig. 5(*c*)

Fig. 5 Instantaneous streamlines corresponding to (*a*) Groove 1 at Re = 780, (*b*) Groove 2 at Re = 700, and (*c*) Groove 3 at Re = 930.

number (±2 percent) and the corresponding frequency of the least-stable mode is presented in Table 2.

Oscillograms for the Groove geometries corresponding to a point located at the center of the main channel are displayed in Fig. 6(*a*). These oscillograms represent the nondimensional u-velocity component as a function of nondimensional time. Notice the repetitive, time-periodic nature of the velocity response. Figure 6(*b*) indicates the result of a Fourier-power analysis conducted for each of the above signals. Although oscillograms for other points in the channel may result in signals with subharmonics and varying coefficient amplitudes, the same fundamental frequency is present.

As the Reynolds number is increased, the amplitude of the mode increases beyond the *small amplitude* assumed in the linear analysis. The mode exhibits a frequency, which has shifted from that corresponding to the critical Reynolds number. This is attributable to nonlinear effects, which are significant for disturbances with finite amplitudes. Such *finite-amplitude* disturbances have been found to differ in frequency from the value predicted by linear stability theory (Orszag and Kells, 1980). However, the traveling wave nature of the instabilities, as well as the close proximity of the obtained frequency to that at criticality, supports the assertion that the channel instabilities are Tollmien-Schlichting instabilities.

The Smount 1 and Smount 2 geometries are investigated to

Table 2 Critical Reynolds numbers and nondimensional frequencies

	Groove 1	Groove 2	Groove 3
Re_c	595	545	710
ω_{TS}	0.523326	0.460287	0.593866
ω_{OF}	0.518502	0.476176	0.592575
Error	0.9219%	3.4519%	0.2173%

ascertain the effect of groove depth upon the amplitude of the traveling waves. As indicated in Table 3, the difference in the frequency of oscillations between these two geometries is negligible, demonstrating the dominance of groove length rather than depth upon frequency selection. However, Smount 1, having a 20 percent deeper groove, exhibits higher amplitude oscillations at the same Reynolds number. This is attributable to the larger portion of the total depth, i.e., groove plus channel depth, that the package constitutes in Smount 1.

Interestingly, Ivtpga, which has the same groove depth as Smount 1, while having the same package height as Smount 2, exhibits the highest amplitude oscillations. This may be due to the momentum contribution of the flow underneath the package (Fig. 4b). However, the relationship between the groove, channel, and under-package flows is complex and requires additional study.

Heat Transfer Enhancement

The benefit of increased exchange of fluid between the channel and the groove is seen clearly by contrasting the stratified isotherms for steady flow (Fig. 7(*a*)) with those corresponding to periodic oscillatory flow (Fig. 7(*b*)). These calculations are performed under the imposition of uniform heat flux along the bottom wall and adiabatic conditions along the top. Local time-dependent, heat transfer coefficients are calculated for each geometry and averaged in time over one wave cycle. The results for both the oscillatory and non-oscillatory cases are displayed graphically, as a function of node number, in Figs. 8 to 10.

A direct relationship becomes apparent by comparing the improvement in the local heat transfer coefficients (Figs. 8 to 10) with the amplitude of the oscillations in the velocity (Fig. 6). Additionally, the same general pattern of enhancement is present. Namely, in all the geometries, the heat transfer coefficients corresponding to the oscillatory flow improve dramatically along the top surface of the package with respect to the steady flow values. This improvement is related to the increase in shear stress associated with the supercritical flow structure. A significant improvement is also realized along the upstream groove bottom and face. These improvements can be attributed to the increase in velocity of the upstream vortex caused by interaction with the traveling waves in the channel. A comparison of the local heat transfer coefficient of each Groove geometry for the nonoscillatory case (Re = 450) is given in Fig. 11. In this case, by increasing the separation between components, increased convective transport is realized. This is a consequence of the vortex structure of the groove flow and a larger shear layer separating the groove and channel flow through which energy may diffuse.

Sample Package

A sample surface-mounted electronic package was constructed to demonstrate the effect of self-sustained oscillatory flows upon the maximum junction temperature. The sample package is based upon a power semiconductor (Harris TO-220), although the heat generation, size, and material properties have been adjusted to those comparable to a small VLSI electronic component. The general configuration is depicted in Fig. 12. Material properties, summarized in Table 4, were

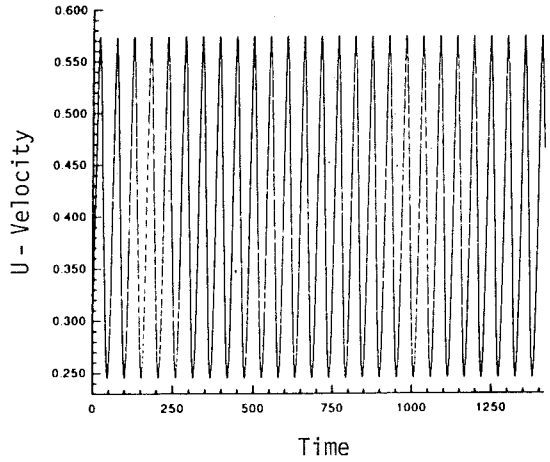

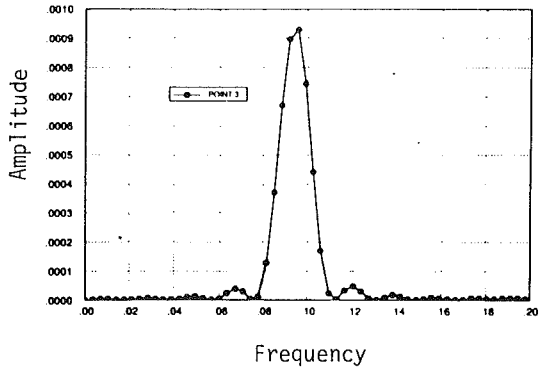

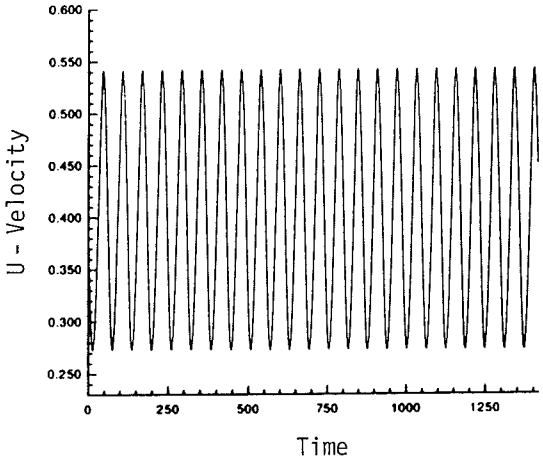

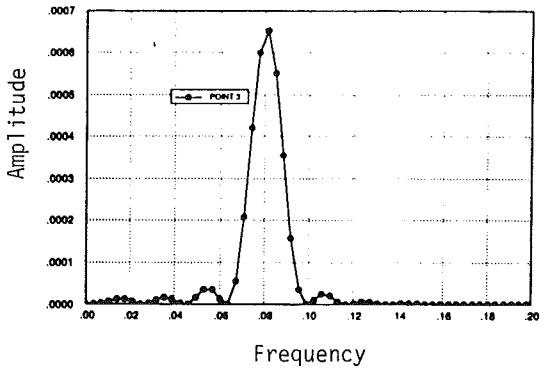

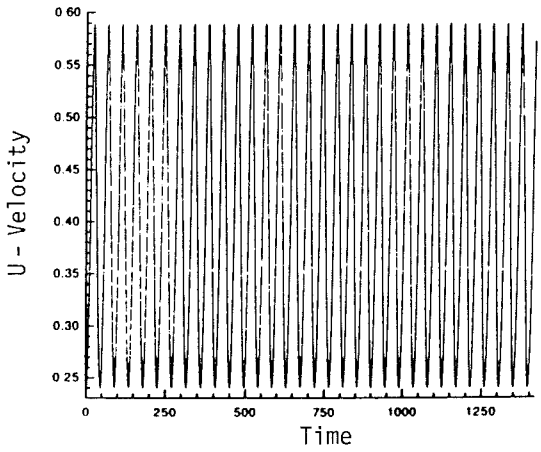

Fig. 6(*a*)

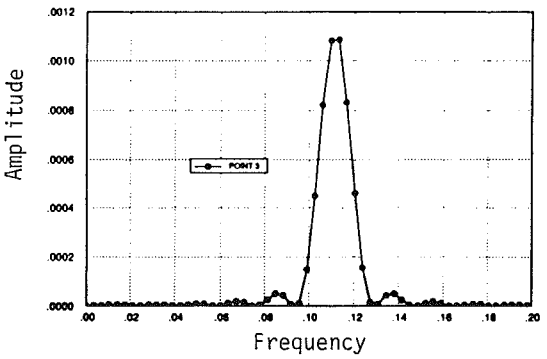

Fig. 6(*b*)

Fig. 6 (*a*) Oscillograms and (*b*) Fourier-power spectra for a characteristic point in Groove 1 at Re = 780, Groove 2 at Re = 700, and Groove 3 at Re = 930, from top to bottom, respectively

selected to both emphasize improved thermal performance and retain realism. In spite of its handling and manufacturing difficulties, Beryllia is used for both the cap and the substrate because of its promise for use in future packages (Pence and Krusius, 1990). A plastic cap is also used to demonstrate the impact of a Beryllia cap upon thermal performance. The chip is specified to dissipate 0.3 Watts of power.

Temperature distributions within the sample package are obtained using the previously calculated, time-averaged, local heat transfer coefficients. For all cases, the heat transfer coefficient along the bottom of the substrate is specified as 0.5 $W/m^2 \cdot °C$. The heat transfer coefficients corresponding to the supercritical case for Groove 3 at Re = 930 are used to calculate the isotherms depicted in Fig. 13(*a*). Additionally, the cap is

Table 3 Frequency and amplitude of oscillations

	Smount 1	Smount 2	Ivtpga
ω_{OF}	0.599259	0.595536	0.586232
Amplitude	5.7211 E-4	4.3289 E-4	6.6555 E-4

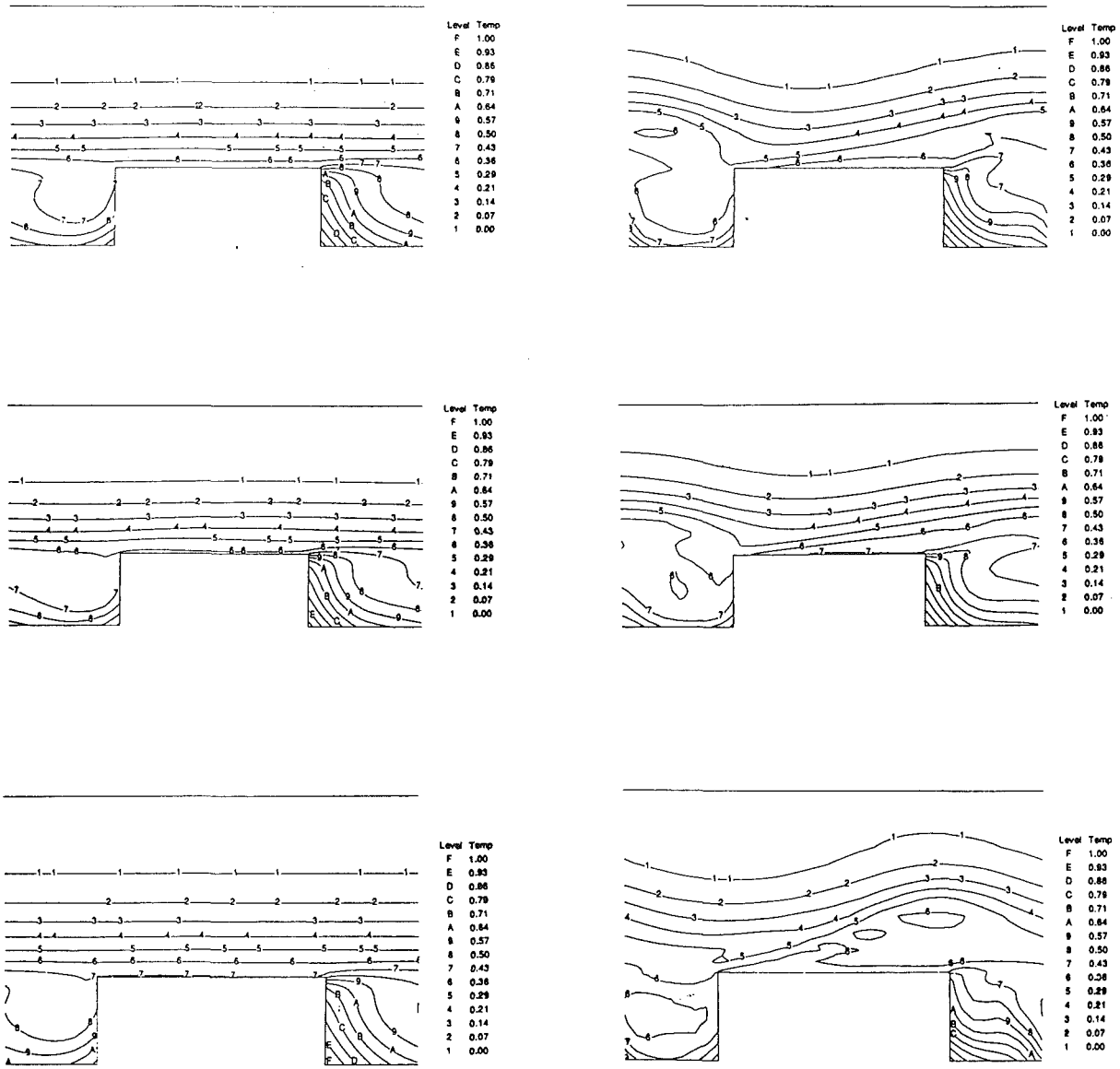

Fig. 7(*a*)

Fig. 7(*b*)

Fig. 7 Isotherms for (a) steady and (b) oscillatory flows, in Groove 1, Groove 2, and Groove 3, from top to bottom, respectively. The isotherms are equally spaced and normalized, from 0 to 1.

composed of plastic. The maximum temperature is 88.55°C and the minimum is 76.13°C, yielding a temperature range of 12.42°C. The isotherms depicted in Fig. 13(*b*) correspond to the local heat transfer coefficients associated with the steady flow regime at Re = 450 with a plastic cap. The corresponding maximum temperature is 119.6°C and the minimum is 108.2°C. The difference in maximum temperatures for the above two flow regimes is significant based on the commonly used criterion in the electronic packaging industry that states that the lifespan of a component is halved for every 10°C increase in junction temperature. Therefore, the supercritical flow pattern would extend the lifespan of the sample component by approximately 800 percent.

To emphasize the significance of using Beryllia as an encapsulant, the temperature field within the package is determined for the supercritical flow with a Beryllia cap. As depicted in Fig. 13(*c*), the maximum temperature is 84.90°C and the minimum is 83.71°C. The use of a Beryllia cap has reduced the maximum temperature by only 3.65°C. However, the temperature range in the package is only 1.19°C, compared to 12.42°C for a plastic cap. Reduction of the internal temperature gradients results in a significant lessening of the thermally-induced stresses sustained inside the electronic package, thereby, demonstrating the advantage of using a Beryllia cap.

Much experimental work has been conducted to determine average heat transfer coefficients (Sparrow et al., 1982; Lehmann and Wirtz, 1985; and Moffat and Ortega, 1988) for grooved-channel geometries in two and three dimensions. However, use of such spatially-averaged heat transfer coefficients in thermal design can result in significantly different temperature predictions. As an example, an average heat transfer coefficient corresponding to the supercritical flow field is calculated and used to generate the isotherms in Fig. 13(*d*). The cap is specified as consisting of plastic material. The maximum temperature obtained is 86.35°C. The difference between the maximum temperatures obtained with the use of average and local values is 1.45°C. However, the predicted temperature range is significantly less by using the spatially-

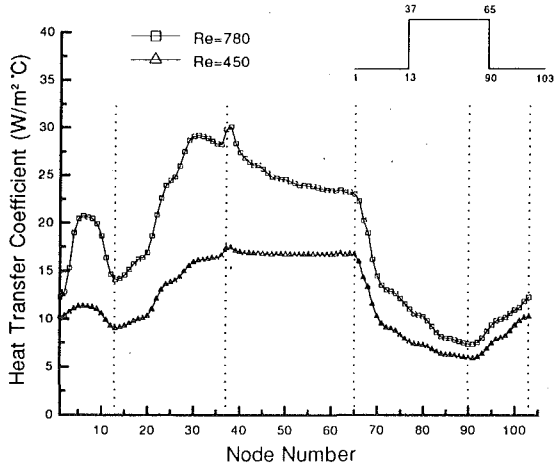

Fig. 8(*a*)

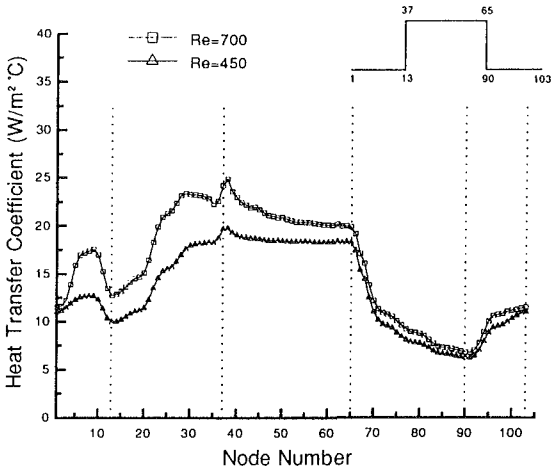

Fig. 8(*b*)

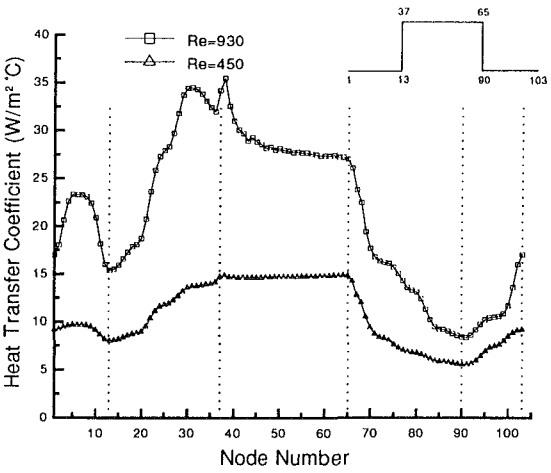

Fig. 8(*c*)

Fig. 8 Local heat transfer coefficient versus node number for (*a*) Groove 1, (*b*) Groove 2, and (*c*) Groove 3

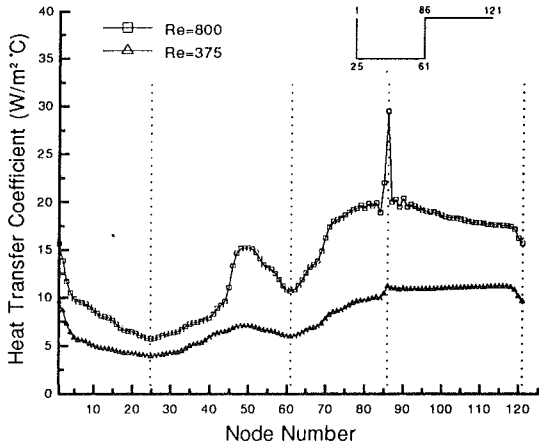

Fig. 9 Local heat transfer coefficient versus node number for Smount 1

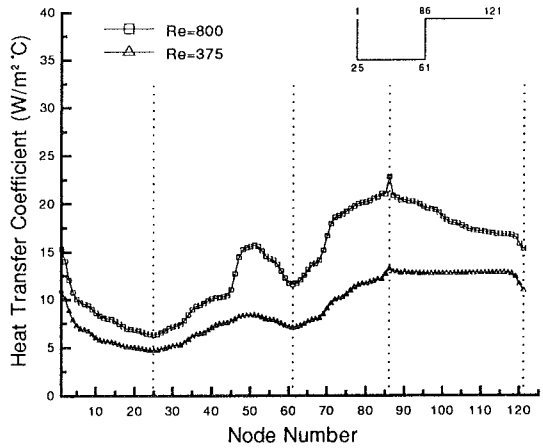

Fig. 10 Local heat transfer coefficient versus node number for Smount 2

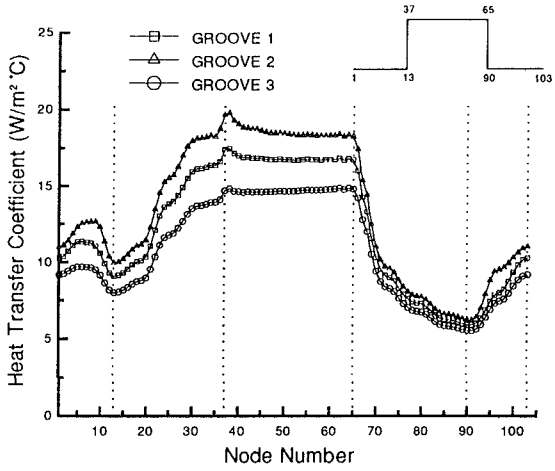

Fig. 11 Local heat transfer coefficient versus node number at Re = 450 for Groove 1, Groove 2, and Groove 3.

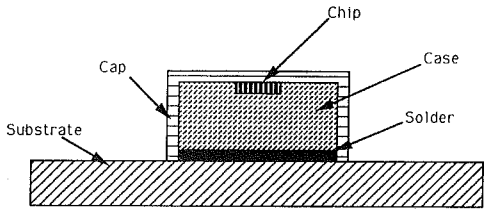

Fig. 12 Schematic of the sample electronic package

averaged heat transfer coefficients. This difference would have a measurable impact on the stress predictions within the package.

For this orientation of surface-mounted components, the highest heat transfer coefficients will exist along the top surface

Table 4 Sample package data

Component	Material	Thermal conductivity Watts/m·C	Width m	Height m
Substrate	Beryllia	218.0	0.0450	0.0072
Solder	Pb-5%Sn	63.0	0.0225	0.0012
Case	Cu Alloy	264.0	0.0225	0.0072
Chip	Si	147.0	0.0050	0.0012
Cap I	Plastic	0.260	0.0012	0.0012
Cap II	Beryllia	218.0	0.0012	0.0012
Fluid	Air@20°C	2.62 E-2	—	—

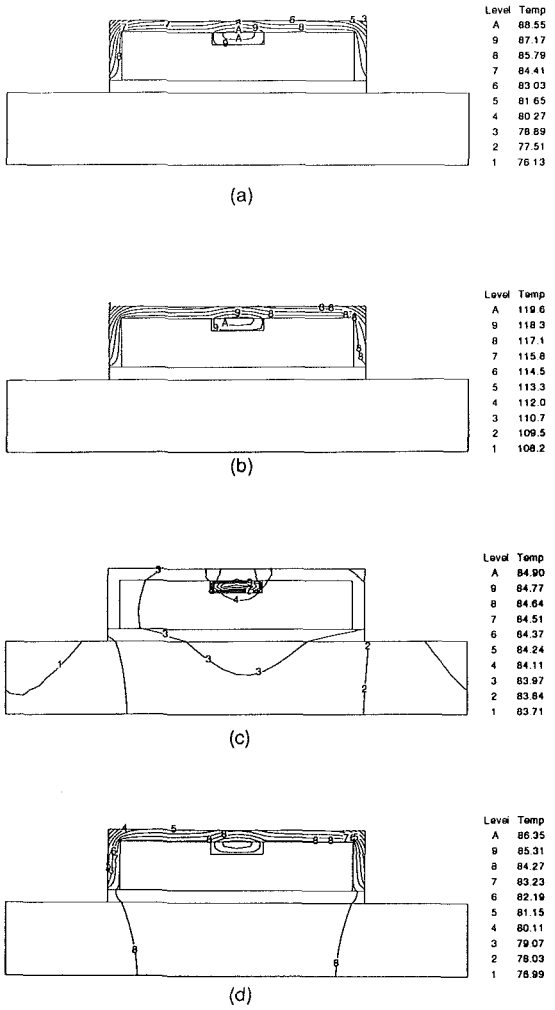

Fig. 13 Temperature distribution in the sample package using local (*a-c*) and spatially averaged heat transfer coefficients (*d*): (*a*) Re = 930, plastic cap, (*b*) Re = 450, plastic cap, (*c*) Re = 930, Beryllia cap, and (*d*) Re = 930, plastic cap

of the package. Therefore, the accuracy of the spatially-averaged heat transfer coefficient is related to the proportion of the total surface area corresponding to the top of the package. In this case, the use of the average value leads to underestimates of maximum temperatures and internal temperature gradients. However, this may not always be so, suggesting that a thermal designer must be careful when using spatially-averaged values for the heat transfer coefficient.

One of the problems confronting a thermal designer is the stringent time constraints associated with the design of commercial electronics in today's highly competitive marketplace. This difficulty can be addressed through the use of a concurrent thermal design methodology, as proposed by Nigen and Amon (1992). However, it is not practical to employ spatially varying heat transfer coefficients throughout the evolution of a design. An additional limitation is the lack of spatially-varying heat transfer coefficients for many of the geometric configurations requiring analysis.

The concurrent design approach utilizes a series of analyses that increase in complexity with the evolution of the design, thereby providing information to the design team, as well as insuring that thermal constraints are satisfied. Initial analyses are conducted using lumped formulations with spatially-averaged heat transfer coefficients. As the design evolves, spatial variability in both the models and boundary conditions is gradually incorporated. When spatially-variable heat transfer coefficients are unavailable, average values are *spatially corrected* to conform to distributions obtained for similar geometric configurations and flow conditions. In this fashion, it is hoped that the high costs and additional time associated with correcting unforeseen flaws, often recognized after production, are reduced. This economizes the design and production processes while increasing overall confidence in the resultant product (Keys et al., 1992).

Conclusion

A numerical investigation of the thermal and fluid behavior of five different grooved-channel geometries, three differing in groove width, two differing in groove depth, and a suspended electronic package, is conducted. The same fundamental flow patterns exist within the grooves for all of the geometries. Likewise, a similar geometric distribution of local heat transfer coefficients is found. This distribution allows for the construction of *spatial correctors* to more accurately account for geometrical variance upon the magnitude of spatially-averaged heat transfer coefficient correlations.

The effectiveness of self-sustained oscillatory flows in enhancing convective cooling of surface-mounted packages is demonstrated through a comparison of maximum junction temperatures. Furthermore, for a typical electronic package, it is found that the use of spatially-averaged heat transfer coefficients leads to significantly different temperature distributions.

Acknowledgment

The authors gratefully acknowledge the support of the Engineering Design Research Center, a National Science Foundation/Engineering Research Center, under cooperative agreement EDC-8943164 and the National Science Foundation Grants CTS-8908808 and CTS-9311072.

References

Amon, C. H., and Patera, A. T., 1989, "Numerical Calculation of Stable Three-Dimensional Tertiary States in Grooved-Channel Flow," *Phys. Fluids A*, Vol. 1, No. 12, pp. 2005–2009.

Amon, C. H., and Mikic, B. B., 1990, "Numerical Prediction of Convective Heat Transfer in Self-Sustained Oscillatory Flows," *J. Thermophysics and Heat Transfer*, Vol. 4, No. 2, pp. 239–246.

Amon, C. H., 1992, "Heat Transfer Enhancement by Flow Destabilization in Electronic Chip Configurations," ASME JOURNAL OF ELECTRONIC PACKAGING, Vol. 114, No. 1, pp. 35–42.

Amon, C. H., Majumdar, D., Herman, C. V., Mayinger, F., Mikic, B. B., and Sekulic, D. P., 1992, "Numerical and Experimental Studies of Self-Sustained Oscillatory Flows in Communicating Channels," *Int. J. Heat Mass Transfer*, Vol. 35, No. 11, pp. 3115–3219.

Azar, K., 1992, "Enhanced Cooling of Electronic Components by Flow Oscillation," *J. Thermophysics and Heat Transfer*, Vol. 6, No. 4, pp. 700–706.

Drazin, P. G., and Reid, W. H., 1981, *Hydrodynamic Stability*, Cambridge, Cambridge University Press, pp. 153–164.

Garimella, S. V., and Eibeck, P. A., 1990, "Heat Transfer Characteristics of an Array of Protruding Elements in Single Phase Forced Convection," *Int. J. Heat Mass Transfer*, Vol. 33, No. 12, pp. 2659–2669.

Ghaddar, N. K., Korczak, K. Z., Mikic, B. B., and Patera, A. T., 1986a, "Numerical Investigation of Incompressible Flow in Grooved Channels. Part 2. Resonance and Oscillatory Heat-Transfer Enhancement," *J. Fluid Mech.*, Vol. 168, pp. 541–567.

Ghaddar, N. K., Magen, M., Mikic, B. B., and Patera, A. T., 1986b, "Numerical Investigation of Incompressible Flow in Grooved Channels. Part 1.

Stability and Self-Sustained Oscillations," *J. Fluid Mech.*, Vol. 163, pp. 99–127.

Greiner, M., 1991, "An Experimental Investigation of Resonant Heat Transfer Enhancement in Grooved Channels," *Int. J. Heat and Mass Transfer*, Vol. 34, No. 6, pp. 1383–1391.

Greiner, M., Chen, R. F., and Wirtz, R. A., 1990, "Heat Transfer Augmentation through Wall-Shape-Induced Flow Destabilization," ASME *Journal of Heat Transfer*, Vol. 112, pp. 336–341.

Karniadakis, G. E., Mikic, B. B., and Patera, A. T., 1988, "Minimum Dissipation Transport Enhancement by Flow Destabilization: Reynolds' Analogy Revisited," *J. Fluid Mech.*, Vol. 192, pp. 365–391.

Kays, W. M., and Crawford, M. E., 1980, *Convective Heat and Mass Transfer*, New York, McGraw-Hill, p. 207.

Keys, K. L., Rao, R., and Balakrishnan, K., 1992, "Concurrent Engineering for Consumer, Industrial Products, and Government Systems," *IEEE Transactions on Comps., Hybrids, and Manuf. Technol.*, Vol. 15, No. 3, pp. 282–287.

Korczak, K. Z., and Patera, A. T., 1986, "An Isoparametric Spectral Element Method for Solution of the Navier–Stokes Equations in Complex Geometry," *J. Comput. Phys.*, Vol. 62, pp. 361–382.

Lehmann, G. L., and Wirtz, R. A., 1985, "The Effect of Variations in Streamwise Spacing and Length on Convection From Surface Mounted Rectangular Components," *Heat Transfer in Electronic Equipment*, ASME-HTD Vol. 48, New York, pp. 39–47.

Leonard, C. T., 1990, "Mechanical Engineering Issues and Electronic Equipment Reliability: Incurred Costs Without Compensating Benefits," *IEEE Transactions on Comps., Hybrids, and Manuf. Technol.*, Vol. 13, No. 4, pp. 895–902.

Moffat, R. J., and Ortega, A., 1988, "Direct Air-Cooling of Electronic Components," *Advances in Thermal Modeling of Electronic Components and Systems*, Vol. 1, A. Bar-Cohen and A. D. Kraus, eds., New York, Hemipshere Publishing Corporation, pp. 129–265.

Nigen, J. S., and Amon, C. H., 1992, "Concurrent Thermal Designs of PCBs: Balancing Time and Accuracy," *IEEE Transactions on Comps., Hybrids, and Manuf. Technol.*, Vol. 15, No. 5, pp. 850–859.

Orszag, S. A., and Kells, L. C., 1980, "Transition to Turbulence in Plane Poiseuille and Plane Couette Flows," *J. Fluid Mech.*, Vol. 96, pp. 159–205.

Patera, A. T., 1984, "A Spectral Element Method for Fluid Dynamics: Laminar Flow in a Channel Expansion," *J. Comp. Phys.*, Vol. 54, pp. 468–477.

Pence, W. E., and Krusius, J. P., 1990, "Package Thermal Resistance: Geometrical Effects in Conventional and Hybrid Packages," *IEEE Transactions on Comps., Hybrids, and Manuf. Technol.*, Vol. 13, No. 2, pp. 245–251.

Ratts, E., Amon, C. H., Mikic, B. B., and Patera, A. T., 1988, "Cooling Enhancement of Forced Convection Air Cooled Chip Array through Flow Modulation Induced by Vortex-Shedding Cylinders in Cross-Flow," *Cooling Technology for Electronic Equipment*, W. Aung., ed., New York, Hemisphere Publishing Company, pp. 183–194.

Schlichting, H., 1979, *Boundary Layer Theory*, New York, McGraw-Hill, pp. 457–465.

Sobey, I. J., 1980, "On Flow Through Furrowed Channels. Part 1. Calculated Flow Patterns," *J. Fluid Mech.*, Vol. 96, pp. 1–26.

Sparrow, E. M., Niethammer, J. E., and Chaboki, A., 1982, "Heat Transfer and Pressure Drop Characteristics of Arrays of Rectangular Modules Encountered in Electronic Equipment," *Int. J. of Heat and Mass Transfer*, Vol. 25, pp. 961–973.

Suzuki, H., Kida, S., Nakamae, T., and Suzuki, K., 1991, "Flow and Heat Transfer Over a Backward-Facing Step with a Cylinder Mounted Near its Top Corner," *Int. J. Heat and Fluid Flow*, Vol. 12, No. 4, pp. 353–359.

U.S.A.F. Rome Air Development Center, 1982, *Handbook for Predictions of Electronic Equipment Reliability*.